J. Phycol. **45,** 787–797 (2009)

DOI: 10.1111/j.1529-8817.2009.00705.x

ULTRASTRUCTURAL CHARACTERIZATION OF THE LYTIC CYCLE OF AN INTRANUCLEAR VIRUS INFECTING THE DIATOM *CHAETOCEROS* CF. *WIGHAMII* (BACILLARIOPHYCEAE) FROM CHESAPEAKE BAY, USA[1]

Yoanna Eissler[2]

Centro de Investigación y Gestión de Recursos Naturales, Departamento de Química y Bioquímica, Facultad de Ciencias, Universidad de Valparaíso, Gran Bretaña 1111, Playa Ancha, Valparaíso, Chile

CIEN Austral, Universidad Austral de Chile, Los Pinos S/N, Balneario Pelluco, Casilla 1327, Puerto Montt, Chile

Kui Wang, Feng Chen

Center of Marine Biotechnology, University of Maryland, 701 East Pratt Street, Baltimore, Maryland 21202, USA

K. Eric Wommack

Delaware Biotechnology Institute, 15 Innovation Way, Newark, Delaware 19711, USA

and D. Wayne Coats

Smithsonian Environmental Research Center, 647 Contees Wharf Road, Edgewater, Maryland 21037, USA

Numerous microalgal species are infected by viruses that have the potential to control phytoplankton dynamics by reducing host populations, preventing bloom formation, or causing the collapse of blooms. Here we describe a virus infecting the diatom *Chaetoceros* cf. *wighamii* Brightw. from the Chesapeake Bay. To characterize the morphology and lytic cycle of this virus, we conducted a time-course experiment, sampling every 4 h over 72 h following viral inoculation. In vivo fluorescence began to decline 16 h after inoculation and was reduced to <19% of control cultures by the end of experiment. TEM confirmed infection within the first 8 h of inoculation, as indicated by the presence of virus-like particles (VLP) in the nuclei. VLP were present in two different arrangements: rod-like structures that appeared in cross-section as paracrystalline arrays of hexagonal-shaped profiles measuring 12 ± 2 nm in diameter and uniformly electron-dense hexagonal-shaped particles measuring ~ 22–28 nm in diameter. Nuclei containing paracrystalline arrays were most prevalent early in the infection cycle, while cells containing VLP increased and then declined toward the end of the cycle. The proportion of nuclei containing both paracrystalline arrays and VLP remained relatively constant. This pattern suggests that rod-like paracrystalline arrays fragmented to produce icosahedral VLP. *C.* cf. *wighamii* nuclear inclusion virus (CwNIV) is characterized by a high burst size (averaged 26,400 viruses per infected cell) and fast generation time that could have ecological implications on *C.* cf. *wighamii* population control.

Key index words: **algal virus; *Chaetoceros*; diatom; viral ecology; virus**

Abbreviations: **CdebDNAV, *Chaetoceros debilis* virus; CsNIV, *Chaetoceros salsugineum* virus; CspNIV, *Chaetoceros* cf. *gracilis* virus; CwNIV, *Chaetoceros* cf. *wighamii* nuclear inclusion virus; FR_{50}, 50% reduction in culture fluorescence; HaNIV, *Heterosigma akashiwo* nuclear inclusion virus; HaRNAV, *H. akashiwo* RNA virus RsRNAV, *Rhizosolenia setigera* virus; VC, viral concentrate; VL, viral lysate; VLP, virus-like particles**

Viruses are widely accepted as playing important roles in the ecology of marine phytoplankton. Most microalgal viruses are lytic and thus have the potential to control phytoplankton dynamics by preventing the formation of blooms (Brussaard 2004) or by spreading rapidly through dense host populations, causing the collapse of blooms (Bratbak et al. 1993, Nagasaki et al. 1994a,b). In addition, inoculation of phytoplankton communities composed of several important algal species using viral concentrates derived from seawater can reduce primary production by as much as 78% (Suttle et al. 1990, Suttle 1992). Viral lysis of phytoplankton and bacteria can also influence biogeochemical cycles by increasing the flux of carbon and nutrients to pools of dissolved and particulate organic matter (Suttle 2005). The emergent impact of viral lysis within marine microbial communities is predicted to be an increase in community respiration and a reduction in the efficiency of carbon transfer to higher trophic levels. Model simulations observed a 33% increase in bacteria respiration and production with

[1]Received 16 May 2008. Accepted 16 March 2009.
[2]Author for correspondence: e-mail yoanna.eissler@uv.cl.

the inclusion of a viral lysis component (Fuhrman 1999). Viral lysis can increase not just carbon availability but other relevant primary nutrients for phytoplankton development such as, P, N, Fe, and Se (Gobler et al. 1997, Poorvin et al. 2004). In addition, viruses can affect the efficiency of the biological pump by converting particulate organic carbon (POC) to dissolved organic carbon (DOC) by cell lysis (i.e., 150 Gt C $\cdot$ year^{-1}) (Suttle 2005), thereby reducing with the rate to which C sinks from surface waters.

Diatoms are among the most important primary producers in the ocean. They are major contributors to global carbon fixation (Dugdale and Wilkerson 1998) and play a predominant role in the biological pump that transfers carbon from surface to deep waters (Eppley and Peterson 1979). Little, however, is known about viruses that infect planktonic diatoms, as most studies have addressed nanophytoplankton-viral systems, with host species usually being representatives of the Prasinophyceae, Prymnesiophyceae, and Pelagophyceae. Among marine planktonic diatoms, the genus *Chaetoceros* is the largest (Rines and Hargraves 1988), being comprised of several hundred described species, with representatives occurring at all latitudes and across estuarine, neritic, and oceanic regions. (Rines and Theriot 2003). Some *Chaetoceros* species can cause fish death due to suffocation or secondary infection, resulting in economic impacts on commercial fisheries (Albright et al. 1992, Harrison et al. 1993, Rensel 1993), although most of them have no negative impact on the ecosystem. Centric diatoms, including *Chaetoceros* species, generally dominate phytoplankton assemblages of Chesapeake Bay (Marshall 1980, 1982, Marshall and Nesius 1996), showing maximum abundance from late winter to early spring (Marshall and Nesius 1996). A recent study reported the isolation of a virus, CspNIV, which infects a common *Chaetoceros* species in the Chesapeake Bay and reaches peak abundances following the annual winter-spring phytoplankton bloom (Bettarel et al. 2005).

To date, four viruses have been reported that infect diatom species. These viruses are characterized by icosahedral morphology, absence of a tail, and small size, varying from 25 to 38 nm. *Rhizosolenia setigera* virus (RsRNAV) (Nagasaki et al. 2004) and *Chaetoceros debilis* virus (CdebDNAV) (Tomaru et al. 2008) replicate within the cytoplasm, whereas *Chaetoceros* cf. *gracilis* virus (CspNIV) (Bettarel et al. 2005) and *Chaetoceros salsugineum* virus (CsNIV) (Nagasaki et al. 2005) replicate within the nucleus. CspNIV forms paracrystalline arrays within the nucleus, apparently distinguishing it from viruses infecting the other three diatoms. These viruses are species-specific and in the case of RsRNAV and CdebDNAV even strain specific. The latent period ranges from 12 to 24 h, 24 h, and 2 d for CsNIV and CdebDNAV, CspNIV, and RsRNAV, respectively. Burst size varies from 55 infection units per host cell for CdebDNAV to 325 infection units per host cell for CsNIV, and 1,010–3,100 infection units per host cell for RsRNAV (burst size was not determined for CspNIV). RsRNAV has a single-stranded RNA genome that is 11.2 kb in length, while CsNIV has a single molecule of covalently closed, circular single-stranded DNA (ssDNA, 6 kb), as well as a segment of linear ssDNA $\sim$ 1 kb, that is complementary to a portion of closed circle creating a partially double-stranded genome. In addition, CdebDNAV has an ssDNA genome. CspNIV was suggested to be an RNA virus based on morphology, but the genome was not characterized. Thus, despite the close phylogenetic relationship of the four diatom hosts, their viruses show marked differences in morphology, infection cycle, and genetic characteristics.

This study reports the isolation and characterization of a new diatom virus from Chesapeake Bay, a nuclear inclusion virus infecting *C.* cf. *wighamii* (CwNIV). CwNIV has several unique biological features that are likely connected with a significant ecological impact of this virus on its diatom hosts in the Bay.

MATERIALS AND METHODS

Algal cultures. The diatom *C.* cf. *wighamii* (Fig. S1, a and b, in the supplementary material) was isolated from Chesapeake Bay using serial dilution of surface water collected at 38°04′ N, 76°13′ W during a cruise onboard the R/V *Cape Henlopen* in October 2004. Unialgal, but nonaxenic, stock cultures were maintained in 16 psu salinity f/2-Si medium (Guillard and Ryther 1962) at 15°C and illuminated with cool-white fluorescent lamps supplying an irradiance of 230 to 300 $\mu E \cdot d^{-1} \cdot m^{-2}$ on a 12:12 light:dark (L:D) cycle. The cultures were gently bubbled by pumping air through silicone tubing connected to a sterile Millipore syringe filter unit of 0.22 μm pore size and 33 mm diameter (PVDF, Millex^{TM}; Millipore Corp., Billerica, MA, USA).

For LM, live specimens were photographed at 1,200X using a Zeiss Axioskop (Carl Zeiss MicroImaging Inc., Göttingen, Germany) equipped for differential interference contrast (DIC). For SEM, specimens were preserved in 1% glutaraldehyde and stored at 4°C until processed. Preserved specimens were concentrated using Millipore membrane filters of 3 μm (25 mm diameter, Isopore membrane, TSTP). The filters were air-dried, sputter-coated with gold-palladium (Model 18930; Ernest F. Fullam Inc., Latham, NY, USA), and examined using a Leo Model 435 VP (Carl Zeiss, Thornwood, NY, USA) scanning electron microscope (Dr. Harold Marshall, personal communication).

Isolation of algal virus. To induce viral infection of *C.* cf. *wighamii*, stock culture was inoculated with viruses concentrated from surface water of Chesapeake Bay (38°58′ N, 76°23′ W). The viral concentrate (VC) was obtained as described by Chen et al. (1996), using water collected on May 7, 2004. To check for the presence of lytic agents, 10 mL of stock culture was dispensed to 20 mL test tubes, inoculated with 1 mL of VC, and incubated as above. Culture aliquots (10 mL) not receiving VC served as controls. After 10 d of incubation, in vivo chl *a* fluorescence of treatments and controls was measured using a Turner Designs 10-AU fluorometer (Turner Designs Inc., Sunnyvale, CA, USA). Treatments showing >50% decrease in fluorescence relative to controls were interpreted as positive for viral lysis. The resultant viral lysate (VL) was filtered through a

0.22 μm pore-size, syringe membrane filter unit and stored at 4°C. The VL was serially diluted with culture medium and added to 10 mL volumes of exponentially growing *C.* cf. *wighamii* to produce duplicate treatments inoculated with the equivalent of 0.5, 0.25, or 0.1 mL of the original lysate. Inoculated cultures and noninoculated controls were incubated for 3 to 5 d under standard growth conditions and then analyzed for in vivo chl fluorescence. The treatment receiving the least amount of VL and showing >50% reduction of in fluorescence relative to controls was filtered as above to produce a second generation VL. This procedure was repeated three times following recommendations of Sandaa et al. (2001), with the final viral lysate designated as CwNIV. CwNIV was then serial transferred >10 times through *C.* cf. *wighamii* culture to propagate VL and enhance the magnitude and timing of culture mortality following inoculation.

Host range analysis. Host specificity of CwNIV was tested by adding VL (5% v/v final concentration) to duplicate cultures (2.5 mL) of algal isolates belonging to the classes Bacillariophyceae, Dinophyceae, Cryptophyceae, Prymnesiophyceae, and Eustigmatophyceae. Cultures were maintained in growth media, incubated at temperatures shown in Table 1, and examined using an inverted microscope (Olympus model IX51; Olympus Corp., Tokyo, Japan) to assess growth and/or lysis of virus inoculated cultures relative to controls inoculated with fresh medium (5% v/v). Cultures not showing lysis after 15 d were considered unsuitable host for the CwNIV.

Virus growth cycle. To follow the infection cycle of CwNIV, 700 mL of *C.* cf. *wighamii* culture in exponential growth was added to each of four 1,000 mL bottles. Two of the bottles received 35 mL of VL, while the other two served as noninoculated controls. VL used to inoculate the cultures was obtained by serial filtration of crude CwNIV lysate through Whatman glass fiber (GF/C then GF/F; 47 mm; Whatman PLC, Kent, UK) and Nucleopore polycarbonate membrane (0.2 μm pore-size; 47 mm diameter; Whatman) filters at a pressure of 130 mm Hg. All bottles were maintained under standard growth conditions and sampled at 4 h intervals over 3 d. At each interval, three samples were taken from each bottle. A 4 mL aliquot was transferred to a 5 mL glass test tube and immediately analyzed for in vivo fluorescence of chl *a* as above. A second, 10 mL sample was preserved with glutaraldehyde (1.25% final concentration) to determine abundance of algae, bacteria, and virus-like particles (VLP). Lastly, a 9 mL sample for TEM was preserved with 1.25% glutaraldehyde (final concentration) in 16 psu estuarine water buffered with 0.05 M sodium cacodylate (pH = 7.4). Preserved samples were stored at 4°C until processed further.

To estimate extracellular viral abundance within culture media, 0.2–0.5 mL of sample was brought up to 1 mL with TE buffer (10 mM Tris and 1 mM EDTA, pH 7.5) and filtered onto 25 mm, 0.02 μm pore-size Anodisc membrane filters (Whatman) at a pressure of 130 mm Hg and stained for 15 min on an 80 μL drop of 2X SYBR-Gold (stock solution = 10,000X, Molecular Probes Inc., Invitrogen Corp., Carlsbad, CA, USA) following methods of Chen et al. (2001). Filters were blotted on a Kimwipe (Kimtech[science], Kimberly-Clark Corp., Neenah, WI, USA) to remove excess fluid, mounted between glass slides and coverslips using 50% spectrophotometric-grade glycerol in 10 mM Tris 1 mM EDTA (pH 7.5), and stored at −20°C until examined. Ten

TABLE 1. Susceptibility of 22 algal strains to CwNIV (*Chaetoceros* cf. *wighamii* nuclear inclusion virus) isolated in the Chesapeake Bay, USA.

Family Genus/species	Cultivation (°C)	Origin of isolation	Strains lysed by CwNIV
Bacillariophyceae			
Navicula lenzi	15	Pond sediment in Eilat Israel	−
Dactyliosolen fragilissimus	15	Chesapeake Bay, Maryland, USA	−
Thalassiosira pseudonana (3H)	15	Moriches Bay, Forge River, Long Island, New York, USA	−
Chaetoceros muelleri	15	North Pacific (21.500 N, 157.833 W)	−
Chaetoceros cf. *gracilis*	15	Rhode River, Maryland, USA	−
Chaetoceros affinis (CCUR)	15	St. Margarets Bay, Nova Scotia, Canada	−
Chaetoceros cf. *tortissimus*	15	Bigelow Lab Dock, West Boothbay Harbor, Maine, USA	−
Chaetoceros laciniosus (3B95E)	15	U. of Rhode Island, Graduate School of Oceanography, Rhode Island, USA	−
Chaetoceros radicans (WCL2)	15	Fladenground, North Sea	−
Chaetoceros socialis (CSOC)	15	Narragasett Bay, Rhode Island, USA	−
Chaetoceros cf. *wighamii*	15	Chesapeake Bay, Maryland, USA	+
Prasinophyceae			
Micromonas pusilla (CCMP9)	15	Bigelow lab dock, West Boothbay Harbor, Maine, USA	−
Dinophyceae			
Karlodinium micrum (CCMP1974)	20	Chesapeake Bay, Maryland, USA	−
Prorocentrum minimum (RR4B1)	20	Rhode River, Maryland, USA	−
Ceratium furca	20	Chesapeake Bay, Maryland, USA	−
Akashiwo sanguinea	20	Chesapeake Bay, Maryland, USA	−
Gyrodinium instriatum	20	Rhode River, Maryland, USA	−
Alexandrium affine	20	Korea	−
Gonyaulax polygramma	20	Korea	−
Cryptophyceae			
Storeatula major	15	Choptank River, Maryland, USA	−
Storeatula major (15 psu)	15	Choptank River, Maryland, USA	−
Prymnesiophyceae			
Isochrysis sp.	15	Chesapeake Bay, Maryland, USA	−
Eustigmatophyceae			
Nannochloropsis sp.	15	Chesapeake Bay, Maryland, USA	−

(−) tested negative for infection, (+) tested positive for infection.

fields were randomly selected to count at least 100 viruses per slide at 1,200X using epifluorescence microscopy (Zeiss Axioscope, filter set #9, excitation BP 450–490, beam splitter FT 510, emission LP 520; Carl Zeiss MicroImaging Inc.).

For determining algal and bacteria abundances, 0.2 to 0.5 mL of sample was concentrated onto an Irgalan Black stained, 0.2 μm pore-size polycarbonate membrane filter (Nucleopore; 25 mm diameter) and stained for 10 min with DAPI (10 $\mu g \cdot mL^{-1}$ final concentration) according to methods of Porter and Feig (1980). Filters were mounted between glass slides and coverslips using low fluorescence immersion oil and stored at –20°C until examined using epifluorescence microscopy (Zeiss Axioscope, filter set # 1, excitation BP 365/12, beam splitter FT 395, emission LP 397). For all samples, a minimum of 100 bacteria and algal cells in at least 10 random fields were counted. Only ''viable'' cells (i.e., those exhibiting DAPI nuclear staining and chl *a* autofluorescence) were enumerated when estimating diatom abundance.

For TEM, preserved cells were pelleted using a Beckman Model 11 microfuge (Beckman Coulter Inc., Fullerton, CA, USA), rinsed with buffer, and postfixed for 2 h in 2% osmium tetroxide in buffer. Pellets were rinsed with distilled water, stained overnight in 2% aqueous uranyl acetate, dehydrated in a graded ethanol series, and transferred through propylene oxide to Spurr's low viscosity embedding medium. Sections 900 to 1,000 μm thick were cut using a diamond knife mounted on a Reichert Ultracut (Reichert-Jung, Vienna, Austria), transferred to uncoated copper grids, and stained with 2% uranyl acetate and 0.02% lead citrate. Ultrathin sections cells were viewed and photographed using a Zeiss EM 10 CA at 80 kV (Carl Zeiss SMT AG, Oberkochen, Germany).

The percent of diatom cells infected by CwNIV was determined by examining 100 arbitrarily selected specimens per sample at ≥120,000X. For estimating burst size of CwNIV, 30 specimens in late-stage infection (time 40 and 44 h) were photographed at 25,000X. Negatives were scanned to tagged image files (TIFF) using Silver Fast software (SilverFast Ai Version 6.1; LaserSoft Imaging AG, Kiel, Germany) and Epson Perfection 4870 photo scanner (Seiko Epson Corporation, Nagano, Japan, Pro Model J131A) and viewed using Zeiss Axiovision (Release 4.3 Carl Zeiss Vision, Hallbergmoos, Germany) with scale calibration. A 2.8 by 2.8 μm grid (each quadrangle = 0.04 μm^2) was placed over displayed images and the number of VLP determined for 10 quadrangles completely occupied by the cell nucleus. VLP $\cdot \mu m^{-3}$ of nucleoplasm was calculated as in Aherne and Dunnill (1982):

$$N_v = \left(\frac{1}{\overline{D}}\right)\overline{N}_A \quad (1)$$

where N_v is the number of VLP per volume of nucleoplasm, $\overline{N}_A$ is the mean number VLP per area of nucleoplasm, and $\overline{D}$ is the mean diameter of VLP. $\overline{D}$ and $\overline{Z}$ were calculated as reported in Aherne and Dunnill (1982):

$$\overline{D} = \frac{\pi}{2\overline{Z}} \quad (2),$$

$$\overline{Z} = \frac{1}{N}\sum\frac{n_i}{d_i} \quad (3)$$

where $\overline{Z}$ is a harmonic mean, N is the total number of VLP profiles measured, n_i is the number of profiles in a given size class, and d_i is profile length of the size class. For this analysis, the 30 negatives examined above were used to measure profile diameter of 1,183 randomly selected VLP, with ≥9 profiles measured per image.

Burst size of CwNIV was then calculated by multiplying VLP $\cdot \mu m^{-3}$ of nucleoplasm by mean volume of *C.* cf. *wighamii* nuclei. To estimate *C.* cf. *wighamii* nuclear volume, images of DAPI-stained specimens were taken at 1,200X using a Carl Zeiss Axiocam (Carl Zeiss MicroImaging Inc.) interfaced with calibrated Axiovision software. Mean nuclear diameter was obtained from measurements of 30 cell nuclei for each sample taken at T40 and T44. Nuclear volume (V) was calculated assuming a spherical shape.

Viral-induced mortality relative to C. *cf.* wighamii *growth rate.* Fifteen experiments were conducted to assess the relationship between *C.* cf. *wighamii* growth rate and the lysis of cultures following viral inoculation. Prior to conducting experiments, growth rate of *C.* cf. *wighamii* was determined following in vivo chl *a* fluorescence sampling once a day, over a maximum of 7 d. For each experiment, 1–3 *C.* cf. *wighamii* cultures (250–700 mL) were inoculated with VL at a final concentration of 5% (v/v) and incubated under standard growth conditions. Cultures were sampled at least once a day for in vivo chl *a* fluorescence as above, with experiments terminated when measurements for inoculated treatments dropped below 20% of initial values. Growth rates for stock cultures and lysis rates of inoculated treatments were determined by fitting the data to an exponential curve using Excel software (edition 2003, Microsoft Corp., Redmond, WA, USA). The lysis rate of inoculated cultures was also used to calculate the time required for viral infection to result in a 50% reduction in culture fluorescence (FR_{50}). Spearman correlation was used to test relationships between growth rate, lysis rate, and FR_{50}.

TEM observation and infectivity of purified viral particles. Sixteen liters of CwNIV algal lysate was concentrated to 400 mL by ultrafiltration using an Amicon Spiral Cartridge Model S1Y30 (30 K, Amicon Corp., Danvers, MA, USA) driven by peristaltic pump ProFlux M12 (Millipore Corp). Polyethylene glycol (PEG 8,000; 100 $g \cdot L^{-1}$ final conc.) was added into the viral concentrate and allowed to completely dissolve overnight at 4°C. The viral particles were then pelleted by centrifugation at 13,870*g* in a Beckman JA-21 rotor (Beckman Coulter) for 30 min. The pellet was cleaned by sequential resuspension in 8 mL TM buffer (20 mL Tris, 10 mM $MgSO_4$) followed by centrifugation. The final viral suspension was mixed with Opti-prep at a final concentration of 40% and ultracentrifuged at 77,738*g* for 20 h using a T-8100 rotor (Sorvall Discovery 100S centrifuge; Thermo Fisher Scientific Inc., Waltham, MA, USA). Visible viral bands were extracted with a needle syringe (gauge 22) and dialyzed three times in 500 mL of SM buffer (100 mM NaCl, 50 mM Tris, 10 mM $MgSO_4$ and 2% gelatin [w/v] pH 7.5) overnight at 4°C. The Opti-prep purified viral suspension was stored at 4°C until further analysis. Then 125 mL of *C.* cf. *wighamii* culture was inoculated with 3 mL of the Opti-prep purified viral suspension to test its infectivity. Samples were taken for TEM analysis as indicated above.

To view free virus particles, a drop of purified viral suspension was placed on a 200-mesh formvar-coated copper grid, stained with aqueous uranyl acetate (0.5%), and then examined and photographed using a Zeiss EM 10 CA operated at 80 kV.

RESULTS

Virus isolate. A pathogen causing lysis of *C.* cf. *wighamii* was successfully isolated from the Chesapeake Bay, USA. The viral pathogen retained algicidal activity after filtration through a 0.22 μm pore-size filter and was serially transferred to exponentially growing *C.* cf. *wighamii* cultures that consistently resulted in lysis. The cultures lysed by the virus turned from brown to a pale green color due to

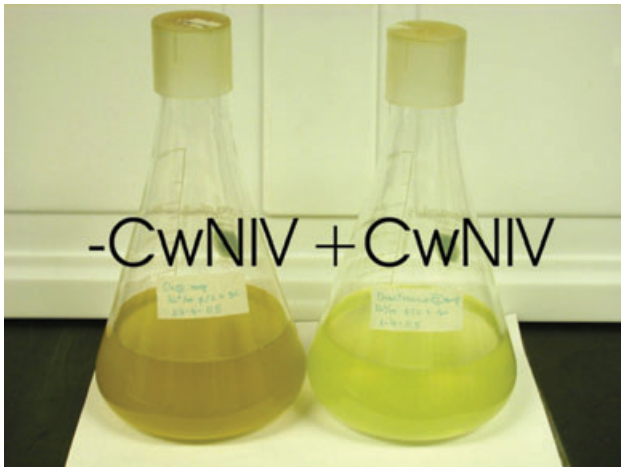

FIG. 1. *Chaetoceros* cf. *wighamii* cultures without (−CwNIV) and with (+CwNIV) CwNIV inoculation.

pigment degradation (Fig. 1). The algal cultures totally crashed after 3–4 d of inoculation with the viral pathogen and did not show regrowth over an additional month-long incubation.

The viral pathogen did not infect or propagate on any of the other algal species tested, including seven species from the same genus, *Chaetoceros*, and three from the same class, Bacillariophyceae. In addition, none of the other species belonging to another five microalgal classes tested was infected; these included 11 different species of flagellate algae (Table 1).

TEM examination of thin section of noninfected *C.* cf. *wighamii* cells indicated that cytoplasmic organization and frustules were typical of diatoms, and there was no indication of the presence of VLP inside the cells (Fig. 2a). TEM preparations of thin-sectioned nuclei of cells inoculated with the virus isolated showed the presence of VLP in two different arrangements. One arrangement consisted of free hexagonal-shaped profiles ~22–28 nm in diameter (average: 25 ± 1.4 nm) that were not uniformly electron dense and lacked a tail. The other arrangement consisted of rod-like arrays that appeared paracrystalline in cross-section with tightly packed hexagonal profiles measuring 12 nm ± 2 SD in diameter (Fig. 2, b and c). In transverse section, rod-like arrays also appeared as fragmented and nonfragmented tubular structures (Fig. 2, b and c). Sections of cell nuclei sometimes contained only rod-like arrays, sometimes only VLP, and sometimes both arrangements (Fig. 2, b–d). Free viral particles observed in viral lysates were hexagonal and averaged 30 nm ± 3 SD in size (Fig. 3a). The Opti-prep purified viruses caused lysis on *C.* cf. *wighamii* culture after 4 d of inoculation. TEM observations of thin sections showed the same virus morphology as described in our time-course study (Fig. 3b). Thus, the purification of the pathogen was completed fulfilling Koch's postulates. The virus infecting *C.* cf. *wighamii* is referred to as CwNIV (nuclear inclusion virus), as it develops inside the host nucleus.

Virus lytic cycle. Following inoculation with CwNIV, in vivo fluorescence and abundance of *C.* cf. *wighamii* cells declined rapidly. Growth of *C.* cf. *wighamii* was inhibited after 8 h of inoculation, and culture decline began 16 h after inoculation (Fig. 4). Inoculated cultures completely crashed by 72 h, with culture fluorescence and *C.* cf. *wighamii* abundance showing an average reduction to 16% (36 [±SE 4] fluorescent units) and 6% (5.8 [±SE 3.6] $\times 10^5$ algal cells $\cdot$ mL^{-1}) of controls values. Control cultures showed a gradual and constant increase in relative in vivo fluorescence (up to 224 [±SE 12] fluorescent units) and an irregular increase of cell abundance (up to 1.02 ± [SE 0.09] $\times 10^7$ algal cells $\cdot$ mL^{-1}). Bacterial densities in inoculated cultures were comparable to the controls, gradually increasing during the experiment, with values ranging from 3.3 (±SE 0.73) $\times 10^7$ to 8.8 (±SE 1.9) $\times 10^7$ bacteria $\cdot$ mL^{-1} (Fig. 5a). Viral abundance remained stable in control cultures through the experiment (average: 5.8 [±SE 0.4] $\times 10^6$ viruses $\cdot$ mL^{-1}) but increased in the infected cultures after 44 h, with values ranging from 0.1 (±SE 0.02) $\times 10^8$ to 1.6 (±SE 0.4) $\times 10^8$ viruses $\cdot$ mL^{-1} at the end of the experiment (Fig. 5b).

TEM observations at 12 h confirmed that over the first 48 h of the experiment there were no VLP inside cell nuclei of control cultures (data not shown). VLP were first detected inside cell nuclei of treatments 4 h after inoculation, representing only 0.5 ± SE 0.5% of cells infected; however, 8 h after inoculation, 5.5% (±SE 3.5) of cells were infected, indicating a short latent period for CwNIV (Fig. 6a). The frequency of infected cells quickly increased to 23.5% (±SE 8.5) at 20 h and then decreased to 15.5% (±SE 0.5) at 32 h, followed by another rise up to 41% (±SE 6.0) at 44 h and subsequent decline to 14% (±SE 2.0) at 52 h of infection (Fig. 6a).

The number of infected cells reached a maximum of 8.9 (±SE 0.45) $\times 10^5$ cells $\cdot$ mL^{-1} at 20 h, gradually decreasing until reaching an average of 1.2 (±SE 0.18) $\times 10^5$ cells $\cdot$ mL^{-1} at 52 h (Fig 6b).

The relative occurrence of different viral arrangements inside nuclei of inoculated *C.* cf. *wighamii* cultures is shown in Figure 7. The percent of infected nuclear profiles containing both VLP and rod-like arrays was relatively uniform throughout the experiment, with an average of 24% (Fig. 7). The percent of infected nuclei containing only rod-like arrays was the highest (61%) at 12 h and tended to decrease over the following 24–28 h, reaching minimum values of 18% (at 40 h). After that, the percent of nuclei containing only rod-like arrays gradually increased through the end of the experiment. The proportion of infected cells containing only VLP was relatively low (average 8%) over 28 h, increasing thereafter to a peak of 60%–62% at 36 to 44 h (Fig. 7). There was a decline in the prevalence of cells with VLP toward

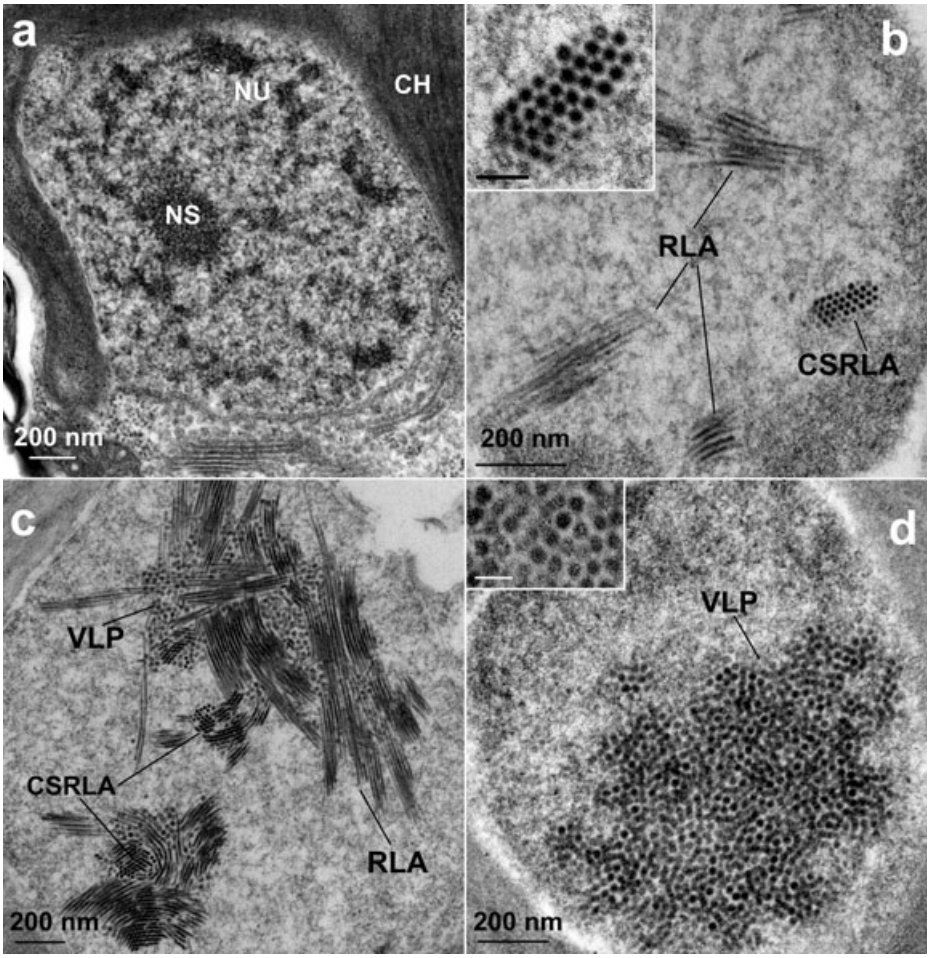

FIG. 2. Transmission electron micrographs of *Chaetoceros* cf. *wighamii*. (a) Thin section of a healthy nucleus (NU: nucleus, NS: nucleolus, CH: chloroplast). (b) Thin section of a cell at early infection, showing rod-like arrays (RLA) and rod-like arrays in cross-section (CSRLA), including an insert for more detail (scale bar, 50 nm). (c) Thin section of a cell at midinfection, showing virus-like particles (VLP), RLA, and CSRLA. (d) Thin section of a cell at late infection, showing VLP, including an insert for more detail (scale bar, 50 nm).

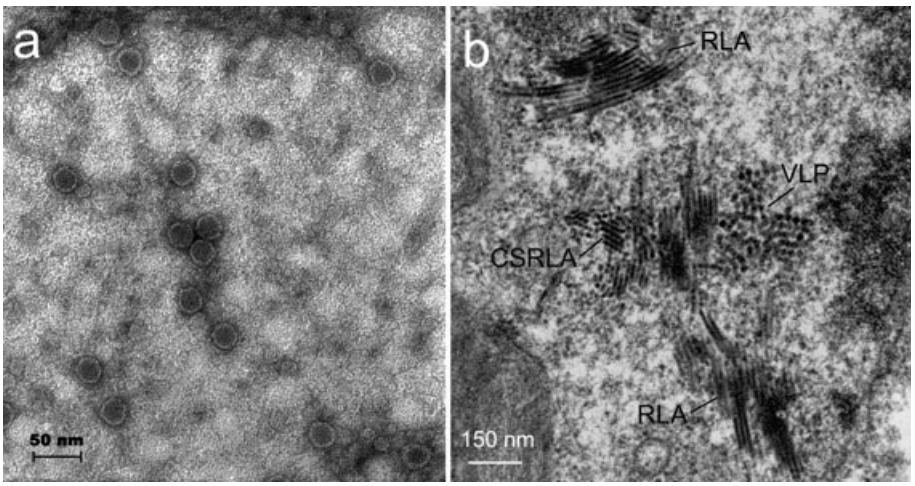

FIG. 3. Transmission electron micrographs showing (a) free viral particles of CwNIV obtained from a viral lysate and (b) thin section of a cell infected with the Opti-prep purified virus, showing VLP, RLA, and CSRLA. RLA, rod-like arrays; CSRLA, rod-like arrays in cross-section; VLP, virus-like particles.

the end of the experiment. Mean values exhibited a clear pattern in the temporal occurrence of viral arrangements, with rod-like arrays more prevalent early in the incubation (8–28 h), replaced by VLP over the following 24 h (Fig. 7).

Burst size of CwNIV determined by TEM morphometry averaged 26,396 (±SE 3,442) viruses per infected cell. Calculations were based on average nuclei volume of 3.6 μm^3, average VLP diameter of 0.02 μm, and a VLP average number of 7,384 (±SE 963) VLP $\cdot$ μm^{-2}.

Viral-induced mortality relative to C. *cf.* wighamii *growth rate.* Growth rate averaged 0.26 (±SE 0.06) $\cdot$ d^{-1} (relative to fluorescence units), showing a range from zero (stationary growth) to 0.64 $\cdot$ d^{-1}. Lytic rate for inoculated cultures averaged 0.42 (±SE

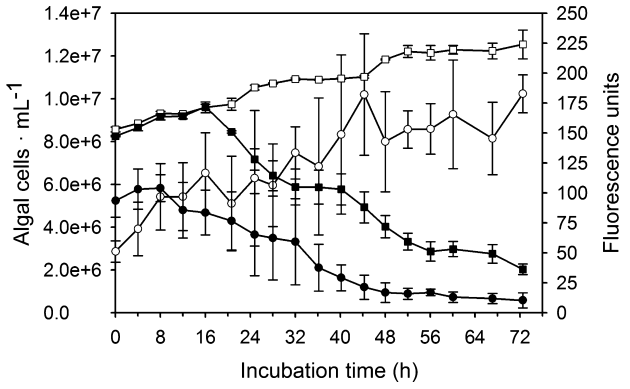

FIG. 4. Infection experiment. Average changes in *Chaetoceros* cf. *wighamii* cell abundance and relative fluorescence units during the experiment for control (white circles: cell abundance; white squares: fluorescence units) and infected cultures (black circles: cell abundance; black squares: fluorescence units). Error bars indicate SE.

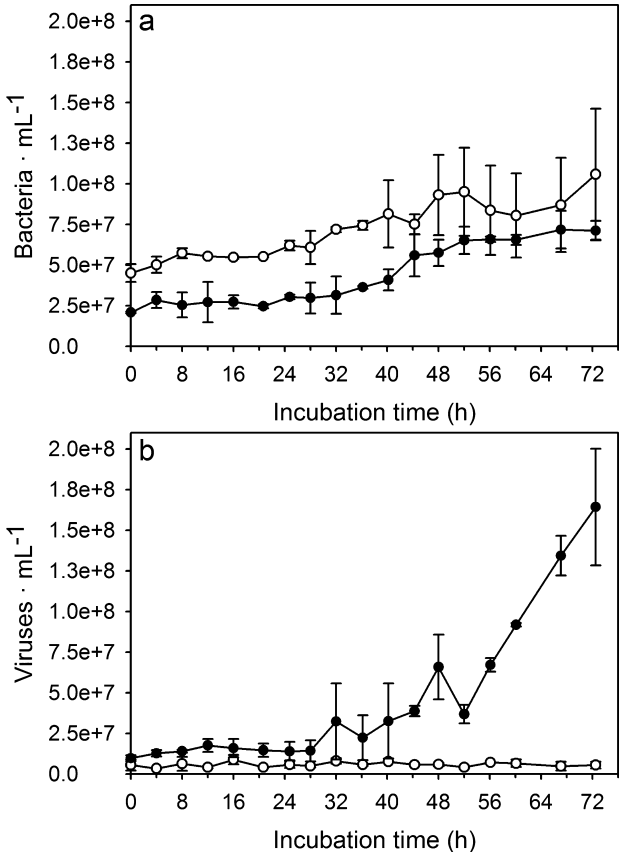

FIG. 5. Infection experiment. (a) Average changes in bacteria abundance during the experiment for control and infected cultures determined by epifluorescence microscopy, using DAPI stain; (b) average changes in viral abundance during the experiment for control and infected cultures determined by epifluorescence microscopy, using SYBR-Gold (white circles stand for control cultures, and black circles stand for infected cultures). Error bars indicate SE.

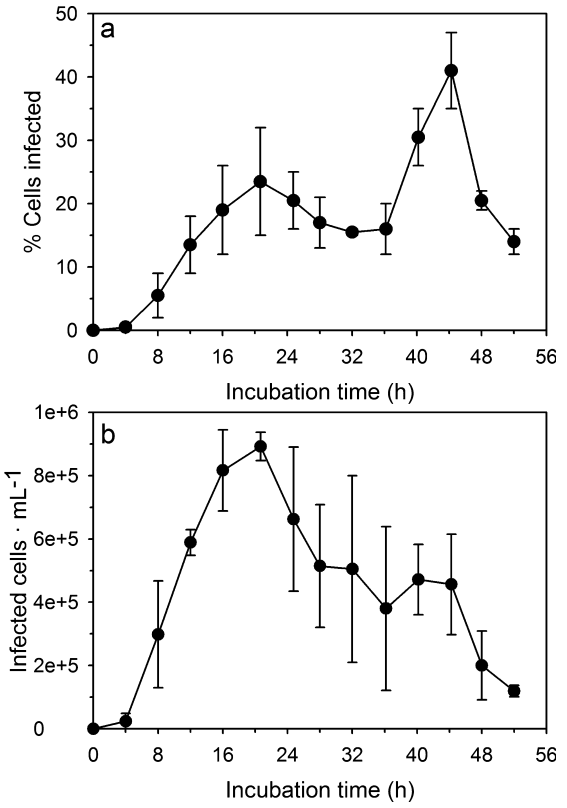

FIG. 6. Infection experiment, TEM images analysis of thin sections of *Chaetoceros* cf. *wighamii* cultures infected with CwNIV. (a) Average percentage of *C.* cf. *wighamii* cells with VLP inside nuclei up to 52 h after inoculation; (b) average number of *C.* cf. *wighamii* cells with VLP inside nuclei up to 52 h after inoculation. Error bars indicate SE. CwNIV, *Chaetoceros* cf. *wighamii* nuclear inclusion virus; VLP, virus-like particles.

0.02) $\cdot d^{-1}$ (range 0.32 to 0.58 $\cdot d^{-1}$), with the time required for 50% reduction in fluorescence (FR_{50}) averaging 2.07 (±SE 0.14) d (range: 1.48 to 3.18 d). Lytic rate and FR_{50} showed no relationship to growth rate as shown in Figure 8. In addition, Spearman correlation showed no relationship among the variables tested (growth rate vs. FR_{50}: $r = 0.05$, $P = 0.86$; growth rate vs. lytic rate: $r = 0.09$, $P = 0.74$).

DISCUSSION

To our knowledge, this is the first report of a virus that forms paracrystalline rod-like arrays inside the nuclei of algal cells. The virus described in this work is the fifth that has been characterized infecting a diatom and the fourth infecting an alga belonging to the genus *Chaetoceros*.

Classification of virus isolated and replication mechanism. The general characteristics of CwNIV are (i) mature particles inside nuclei that are hexagonal in shape and small in size, average 25 ± 1.4 nm in diameter, with free viral particles averaging 30 ± 3 nm and having an hexagonal shape; (ii) replication occurring within the nucleus of the host

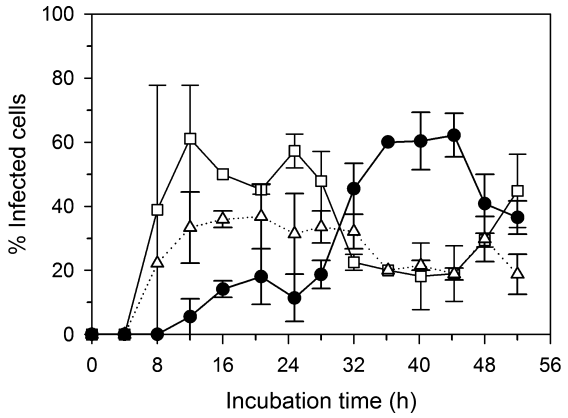

FIG. 7. Infection experiment, TEM images analysis of thin sections of *Chaetoceros* cf. *wighamii* cultures infected with CwNIV. Average frequency of paracrystalline arrays and VLP inside *C.* cf. *wighamii* nuclei. Error bars indicate SE. White squares stand for % of paracrystalline arrays, white triangles stand for % paracrystalline arrays and VLP, and black circles stand for VLP only. CwNIV, *Chaetoceros* cf. *wighamii* nuclear inclusion virus; VLP, virus-like particles.

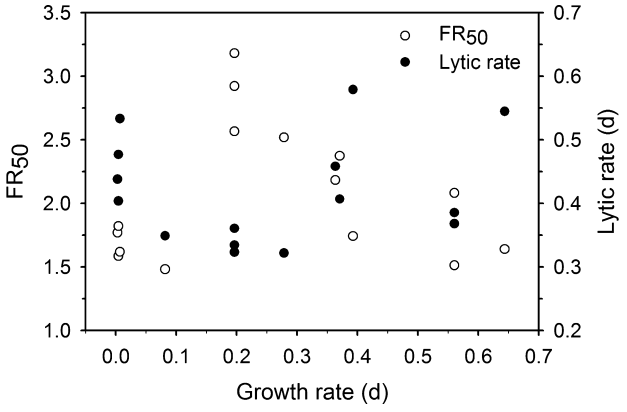

FIG. 8. Relationship between growth rate and 50% reduction in culture fluorescence (FR_{50}) and lytic rate on 15 infection experiments conducted.

cell; and (iii) formation of closely packed rod-like arrays inside the host nuclei.

The earliest algal viruses described in the literature belong to the family Phycodnaviridae (Van Etten 1995), members of which specifically infect eukaryotic algae. Phycodnaviridae are polyhedral in shape, 100–200 nm in diameter, do not have an envelope, lack a tail, contain large double-stranded DNA genomes ranging from 100 to 560 kbp, and proliferate in the cytoplasm (see review Brussaard 2004). According to these characteristics, CwNIV clearly does not belong to the Phycodnaviridae.

Nuclei containing paracrystalline rod-like arrays were most prevalent early in the infection cycle, while cells containing VLP increased and then declined toward the end of the cycle. By contrast, the proportion of nuclei containing both paracrystalline arrays and VLP remained relatively constant. The oscillating pattern observed for percent cells infected and morphologically distinct viral configurations (Fig. 7) suggests that rod-like arrays fragment with maturation, producing hexagonal VLP. This type of viral replication or the presence of paracrystalline rod-like arrays has never been reported for any virus infecting eukaryotic marine or freshwater algae. However, it is necessary to point out that the size determined in cross-section for paracrystalline rod-like arrays is smaller than the size for mature VLP, which could support an alternative hypothesis of the coinfection of two different viruses or, as was suggested, the presence of an incomplete stage of maturation of the same virus. Several rod-shape viruses, however, have been reported to infect vascular plants, including species belonging to the families tobravirus, tobamovirus, furovirus, and hordeivirus (Matthews 1991). The replication of those viruses involves the appearance of different morphological stages during maturation of the viruses, but only mature rod-shape viruses are produced. However, the *Solanum nodiflorum* mottle virus (SNMV), which infects a common weed in eastern Australia, is hexagonal, 28 nm in diameter, and was found in association with tubular and rod-shaped structures inside the nuclei. Therefore, the developmental pattern reported here for CwNIV is not without precedent. Nevertheless, the fact that paracrystalline rod-like arrays increase toward the end of the cycle and VLP decrease may imply, as was already suggested, that these are two different viruses infecting *C.* cf. *wighamii* at the same time (one hexagonal and one rod-like). However, rod-like viruses were never observed in viral lysates. Consequently, one explanation is that the only morphological stage of maturation for CwNIV particles that are released from the cells is mature VLP.

Maturation of viral particles in plants has been described in association with the endoplasmic reticulum, nucleus, and chloroplast, among other organelles, and involves a series of cytological changes, such as the formation of large regions in the cytoplasm of infected cells, known as viroplasm, where mature virus particles appear in membrane-bound sacs (e.g., barley yellow striate mosaic virus) (Matthews 1991). For algal viruses, two areas of viral assembly have been reported. The cytoplasm has been reported for members of the Phycodnaviridae, one ssRNA virus infecting *Heterosigma akashiwo*, HaRNAV (Tai et al. 2003), and the two diatom viruses RsRNAV and CdebDNAV, which infect *R. setigera* and *C. debilis*, respectively (Nagasaki et al. 2004, Tomaru et al. 2008) (Table 2). The nucleus has been reported for two viruses, CsNIV and CspNIV, that infect *C. salsugineum* and *C.* cf. *gracilis*, respectively (Bettarel et al. 2005, Nagasaki et al. 2005), and HaNIV, which infects *H. akashiwo* (Lawrence et al. 2001) (Table 2). For CwNIV, only the nucleus is involved in the assembly of viral particles, since

TABLE 2. Comparison among viruses infecting diatoms and two viruses that infect *Heterosigma akashiwo*.

Family Species	Bacillariophyceae *Chaetoceros* cf. *wighamii*	Bacillariophyceae *Chaetoceros* cf. *gracilis*	Bacillariophyceae *Chaetoceros salsugineum*	Bacillariophyceae *Chaetoceros debilis*	Bacillariophyceae *Rhizosolenia setigera*	Rhaphidophyceae *Heterosigma akashiwo*	
Virus family	n.d.	n.d.	n.d.[a]	n.d.	n.d.	n.d.	n.d.
Genome type	n.d.	n.d.	Circular ssDNA + linear segment ssDNA	ssDNA	ssRNA	n.d.	ssRNA
Genome size (kbp)	7–8	n.d.	6, ~1, respectively	7, 5, 1.4, and 0.8	11.2	n.d.	9.1
Particle type	Icosahedral	Icosahedral	Icosahedral	Icosahedral	Icosahedral	Icosahedral	Icosahedral
Particle size (nm)	25, 30[b]	25	38	30	32	30	25
Latent period (h)	8	24	12–24	12–24	48	24	48
Virus proliferation	Nucleus	Nucleus	Nucleus	Cytoplasm	Cytoplasm	Nucleus	Cytoplasm
Paracrystaline arrays	Yes	Yes	No	No	No	Yes	Yes
Burst size (# per cell)	26,396	n.d.	325	55	3,100, 1,010[c]	10,000	n.d.
Location of isolation	Chesapeake Bay, USA	Rhode River, Chesapeake Bay, USA	Shiotsuka River, Ariake Sea, Japan	Western Japan	Ariake Sea, Japan	Jericho Beach, BD, Canada	Fraser River plume, Strait of Georgia, BC, Canada
References	This article	Bettarel et al. 2005	Nagasaki et al. 2005	Tomaru et al. 2008	Nagasaki et al. 2004, Shirai et al. 2006	Lawrence et al. 2001	Tai et al. 2003

n.d., not determined.
[a]Similar to Circoviruses.
[b]Average of particle size inside nuclei and free viral particles in lysate, respectively.
[c]Inoculation of the cultures during exponential and stationary phases, respectively.

there was no indication of viruses or paracrystalline rod-like arrays in any other area of infected cells. The nuclear inclusion viruses share some similar characteristics, including small size (<40 nm in diameter), small genome (<10 kb), and, except for CsNIV, formation of paracrystalline arrays inside the nuclei of infected cells (Table 2). However, formation of paracrystalline arrays in these other viruses corresponds to the alignment of icosahedral viral particles that appear as a continuous mass or layer of particles (Lawrence et al. 2001, Bettarel et al. 2005). Regarding this possibility, formation of paracrystalline arrays might be a common feature of viruses that are assembled inside the nucleus of algal cells. However, it has been reported that HaRNAV, which develops in the cytoplasm, forms crystalline arrays where the particles are presented as complete or incomplete VLP (Tai et al. 2003).

Virus lytic cycle. The latent period for CwNIV is 8 h, which is in the range of 3–48 h reported for the viruses within the Phycodnaviridae (Brussaard 2004). Comparison with other small algal viruses shows that CwNIV exhibits the shortest latent period (Table 2). It has been proposed that viruses can act as microbial controls restricting the growth of phytoplankton populations (Brussaard 2004). Therefore, the highly lytic action of CwNIV could prevent *C.* cf. *wighamii* from being abundant in the environment. In fact, *C.* cf. *wighamii* has been reported in the Chesapeake Bay as rare (Wass 1972) or not present (Marshall 1980, 1982, Marshall and Nesius 1996). Rare detection, however, could be due to the very small size of *C.* cf. *wighamii* (apical axis 7–18 μm as reported in Tomas 1997), which makes identification of this species difficult.

The percentage of cells with VLP showed mainly one peak, after 32 h of inoculation, suggesting one cycle of VLP production. Similarly, *H. akashiwo* showed maximum prevalence 74 h postinfection with HaNIV, with 98% of the cells being infected (Lawrence et al. 2001).

Ecological implications. CwNIV appears to be host-specific as none of the other 21 algal species tested was infected, including 10 Bacillariophyceae, seven of which belonged to the genus *Chaetoceros*. Interestingly, one of the noninfected algae was *C.* cf. *gracilis*, a small diatom inhabiting Chesapeake Bay for which a nuclear inclusion virus resembling CwNIV has been isolated (i.e., CspNIV, Bettarel et al. 2005). Among diatoms, viruses typically are not only species-specific but also strain specific, such as RsRNAV (Nagasaki et al. 2004) and CdebDNAV (Tomaru et al. 2008). The specificity of diatom viruses like CwNIV suggests that viral strains are intricately linked to their host populations, thereby differentially influencing the formation and persistence of blooms in nature.

Burst size of CwNIV based on analysis of TEM images averaged 26,400 viruses per infected cell, which is considerably higher than previously

estimated for diatom viruses (see Table 2) and algal viruses within the Phycodnaviridae (Van Etten 1995), where not more than a hundred viral particles are produced per host cell. However, CwNIV burst size is similar to a nuclear inclusion virus that forms chrystalline arrays when infecting *H. akashiwo* (Lawrence et al. 2001). Lawrence et al. (2001) postulated that production of crystalline arrays could have ecological implications. As infected host cells lyse, the release of crystalline viral arrays would decrease viral dispersal and host reinfection (Lawrence et al. 2001). Alternatively, crystalline arrays might make the viruses more persistent in the environment. CwNIV, however, did not show paracrystalline structures in viral lysate, suggesting that only free virus particles are released to the environment. For CwNIV, the release of a large number of free viral particles, rather than a few paracrystalline arrays, may increase the likelihood of host-viral contact and provide a special advantage in the marine environment where microturbulence affects particle behavior. Particle size and motility are important properties that can affect infection mechanisms, since infection depends on random encounters between virus and host cells (Murray and Jackson 1992). Consequently, the size of algal viruses is an important characteristic, and in the case of diatom viruses, small size (i.e., <40 nm in diameter) is a shared feature (Table 2). Such an attribute may facilitate their entrance into the host cells through the pores located in the host frustule, as has been previously suggested for *R. setigera* since the pores are larger than RsRNAV (Nagasaki et al. 2004). An alternative for *C. salsugineum* would be that CsNIV could enter the cells through ellipse pores located on the setae since frustule pores are smaller than CsNIV (Nagasaki et al. 2005).

Lytic rates of *C.* cf. *wighamii* cells after viral inoculation were similar irrespective of culture growth phase, indicating a lack of host density dependence for successful virus infection. Typically, infection of host cells during stationary growth phase results in decreased burst size, indicating an interaction between host physiological condition and viral production (Van Etten et al. 1991, Bratbak et al. 1998). For CwNIV, however, the physiological condition of host cells appears to have little or no affect on the infection process.

CONCLUSION

CwNIV is an icosahedral virus, lacking a tail and having a capsid size ranging from 25 to 30 nm, as previously described for diatom viruses (Nagasaki et al. 2004, 2005, Bettarel et al. 2005, Tomaru et al. 2008). According to our findings, CwNIV maturation most likely involves formation of rod-like structures that appear in cross-section as paracrystalline arrays that fragmented to produce icosahedral VLP. This developmental pattern has not been described for any other eukaryotic marine or freshwater algal virus. However, the discussion remains open as to the alternative hypothesis of two different viruses coinfecting the same cell (one hexagonal and one rod-like). Burst size of CwNIV based on analysis of TEM images averaged 26,400 viruses per infected cell, similar to the burst size of *H. akashiwo* nuclear inclusion virus (Table 2). CwNIV is species-specific, as are the majority of known algal viruses.

We thank Drs. Richard V. Lacouture and Marie Anne Hartsig for their help in identification of *Chaetoceros* species and for providing microalgal cultures. We are also grateful to Dr. Harold Marshall for providing SEM images used in this study. This research was supported by National Science Foundation grant MCB-0132070 to K. E. W., F. C., D. W. C.

Aherne, W. A. & Dunnill, M. S. 1982. *Morphometry*. Edward Arnold (Publishers) Ltd., London, 206 pp.

Albright, L. J., Johnson, S. & Yousif, A. 1992. Temporal and spatial distribution of the harmful diatoms *Chaetoceros concavicornis* and *Chaetoceros convolutus* along the British Columbia coast. *Can. J. Fish. Aquat. Sci.* 49:1924–31.

Bettarel, Y., Kan, J., Wang, K., Williamson, K. E., Cooney, S., Ribblett, S., Chen, F., Wommack, K. E. & Coats, D. W. 2005. Isolation and preliminary characterisation of a small nuclear inclusion virus infecting the diatom *Chaetoceros* cf. *gracilis*. *Aquat. Microb. Ecol.* 40:103–14.

Bratbak, G., Egge, J. K. & Hendal, M. 1993. Viral mortality of the marine alga *Emiliana huxleyi* (Haptophyceae) and termination of algal blooms. *Mar. Ecol. Prog. Ser.* 93:39–48.

Bratbak, G., Jacobsen, A., Heldal, M., Nagasaki, K. & Thingstad, F. 1998. Virus production in *Phaeocystis pouchetii* and its relation to host cell growth and nutrition. *Aquat. Microb. Ecol.* 16: 1–9.

Brussaard, C. P. D. 2004. Viral control of phytoplankton populations – a review. *J. Eukaryot. Microbiol.* 51:125–38.

Chen, F., Lu, J. R., Binder, B. J., Liu, Y. C. & Hodson, R. E. 2001. Application of digital image analysis and flow cytometry to enumerate marine viruses stained with SYBR gold. *Appl. Environ. Microbiol.* 67:539–45.

Chen, F., Suttle, C. A. & Short, S. M. 1996. Genetic diversity in marine algal virus communities as revealed by sequence analysis of DNA polymerase genes. *Appl. Environ. Microbiol.* 62:2869–74.

Dugdale, R. C. & Wilkerson, F. P. 1998. Silicate regulation of new production in the equatorial Pacific upwelling. *Nature* 391:270–3.

Eppley, R. W. & Peterson, B. J. 1979. Particulate organic matter flux and planktonic new production in the deep ocean. *Nature* 282:677–80.

Fuhrman, J. A. 1999. Marine viruses and their biogeochemical and ecological effects. *Nature* 399:541–8.

Gobler, C. J., Hutchins, D. A., Fisher, N. S., Cosper, E. M. & Sanudo-Whilhelmy, S. 1997. Release and bioavailability of C, N, P, Se, and Fe following viral lysis of a marine Chrysophyte. *Limnol. Oceanogr.* 42:1492–504.

Guillard, R. R. L. & Ryther, J. H. 1962. Studies on marine planktonic diatoms. I. *Cyclotella nana* Hustedt and *Detonula confervacea* (Cleve) Gran. *Can. J. Microbiol.* 8:229–39.

Harrison, P. J., Thompson, P. A., Guo, M. & Taylor, F. J. R. 1993. Effects of light, temperature and salinity on the growth rate of harmful marine diatoms, *Chaetoceros convolutus* and *C. concavicornis* that kill netpen salmon. *J. Appl. Phycol.* 5:259–65.

Lawrence, J. E., Chan, A. M. & Suttle, C. A. 2001. A novel virus (HaNIV) causes lysis of the toxic bloom-forming alga *Heterosigma akashiwo* (Rhaphidophyceae). *J. Phycol.* 37:216–22.

Marshall, H. G. 1980. Seasonal phytoplankton composition in the lower Chesapeake Bay and Old Plantation Creek, Cape Charles, Virginia. *Estuaries* 3:207–16.

Marshall, H. G. 1982. The composition of phytoplankton within the Chesapeake Bay plume and adjacent waters off Virginia Coast, U.S.A. *Estuar. Coast. Shelf Sci.* 15:29–43.
Marshall, H. G. & Nesius, K. K. 1996. Phytoplankton composition in relation to primary production in Chesapeake Bay. *Mar. Biol.* 125:611–7.
Matthews, R. E. F. 1991. *Plant Virology*, 3rd ed. Academic Press, San Diego, California, 835 pp.
Murray, A. G. & Jackson, G. A. 1992. Viral dynamics: a model of the effects of size, shape, motion and abundance of single-celled planktonic organisms and other particles. *Mar. Ecol. Prog. Ser.* 89:103–16.
Nagasaki, K., Ando, M., Imai, I., Itakura, S. & Ishida, Y. 1994a. Virus-like particles in *Heterosigma akashiwo* (Rahidophyceae): a possible red tide disintegration mechanism. *Mar. Biol.* 119:307–12.
Nagasaki, K., Ando, M., Itakura, S., Imai, I. & Ishida, Y. 1994b. Viral mortality in the final stage of *Heterosigma akashiwo* (Rahidophyceae) red tide. *J. Plankton Res.* 16:1595–9.
Nagasaki, K., Tomaru, Y., Katanozaka, N., Shirai, Y., Nishida, K., Itakura, S. & Yamaguchi, M. 2004. Isolation and characterisation of a novel single-stranded RNA virus infecting the bloom-forming diatom *Rhizosolenia setigera*. *Appl. Environ. Microbiol.* 70:704–11.
Nagasaki, K., Tomaru, Y., Takao, Y., Nishida, K., Shirai, Y., Suzuki, H. & Nagumo, T. 2005. Previously unknown virus infects marine diatom. *Appl. Environ. Microbiol.* 71:3528–35.
Poorvin, L., Rinta-Kanto, J. M., Hutchins, D. A. & Wilhelm, S. W. 2004. Viral release of iron and its bioavailability to marine plankton. *Limnol. Oceanogr.* 49:1734–41.
Porter, K. G. & Feig, T. S. 1980. The use of DAPI for identifying and counting aquatic microflora. *Limnol. Oceanogr.* 25:943–8.
Rensel, J. E. 1993. Severe blood hypoxia of Atlantic salmon (*Salmo salar*) exposed to the marine diatom *Chaetoceros concavicornis*. *In* Smayda, T. J. & Shimizu, Y. [Eds.] *Toxic Phytoplankton Blooms in the Sea*. Elsevier, New York, pp. 625–30.
Rines, J. E. B. & Hargraves, P. E. 1988. The *Chaetoceros* Ehrenberg (Bacillariophyceae) flora of Narragansett Bay, Rhode Island, U.S.A. *Bibl. Phycol.* 79:1–196.
Rines, J. E. B. & Theriot, E. C. 2003. Systematics of Chaetocerotaceae (Bacillariophyceae). I. A phylogenetic analysis of the family. *Phycol. Res.* 51:83–98.
Sandaa, R. A., Heldal, M., Castberg, T., Thyrhaug, R. & Bratbak, G. 2001. Isolation and characterization of two viruses with large genome size infecting *Chrysochromulina ericina* (Prymnesiophyceae) and *Pyramimonas orientalis* (Prasinophyceae). *Virol* 290:272–80.
Shirai, Y., Takao, Y., Mizumoto, H., Tomaru, Y., Honda, D. & Nagasaki, K. 2006. Genomic and phylogenetic analysis of a single-stranded RNA virus infecting the bloom-forming diatom *Rhizosolenia setigera*. *J. Mar. Biol. Assoc. U. K.* 86:475–83.
Suttle, C. A. 1992. Inhibition of photosynthesis in phytoplankton by the submicron size fraction concentrated from seawater. *Mar. Ecol. Prog. Ser.* 87:105–12.
Suttle, C. A. 2005. Viruses in the sea. *Nature* 437:356–61.
Suttle, C. A., Chan, A. M. & Cottrell, M. T. 1990. Infection of phytoplankton by viruses and reduction of primary productivity. *Nature* 347:467–9.
Tai, V., Lawrence, J. E., Lang, A. S., Chan, A. M., Culley, A. I. & Suttle, C. A. 2003. Characterization of HaRNAV, a single-stranded RNA virus causing lysis of *Heterosigma akashiwo* (Raphidophyceae). *J. Phycol.* 39:343–52.
Tomaru, Y., Shirai, Y., Suzuki, H., Naguno, T. & Nagasaki, K. 2008. Isolation and characterization of a new single-stranded DNA virus infecting the cosmopolitan marine diatom *Chaetoceros debilis*. *Aquat. Microb. Ecol.* 50:103–12.
Tomas, C. R. 1997. *Identifying Marine Phytoplankton*, 1st ed. Academic Press, San Diego, California, 858 pp.
Van Etten, J. L. 1995. Phycodnaviridae. *In* Murphy, F. A., Fauguet, C. M., Bishop, D. H. L., Ghabrial, S. A., Jarvis, A. W., Martelli, G. P., Mayo, M. A. & Summers, M. D. [Eds.] *Virus Taxonomy*. Springer-Verlag, Vienna, Austria, pp. 100–3.
Van Etten, J. L., Lane, L. C. & Meints, R. H. 1991. Viruses and virus like particles of eukaryotic algae. *Microbiol. Rev.* 55: 586–620.
Wass, M. L. 1972. *A Check List of the Biota of the Lower Chesapeake Bay*. Special Scientific Report No. 65. Virginia Institute of Marine Science, Gloucester Point, Virginia, 290 pp.

Supplementary Material

The following supplementary material is available for this article:

Figure S1. *C.* cf. *wighamii*: (a) optical microphotograph of healthy cells; (b) scanning electron microphotograph of healthy cells.

This material is available as part of the online article.

Please note: Wiley-Blackwell are not responsible for the content or functionality of any supporting materials supplied by the authors. Any queries (other than missing material) should be directed to the corresponding author for the article.